Robust laser beam engineering using polarization and angular momentum diversity

Article *in* Optics Express · July 2017

DOI: 10.1364/OE.25.017524

CITATIONS
26

READS
310

3 authors:

Priyanka Lochab
Indian Institute of Technology Delhi
19 PUBLICATIONS **92** CITATIONS
SEE PROFILE

P. Senthilkumaran
Indian Institute of Technology Delhi
231 PUBLICATIONS **2,461** CITATIONS
SEE PROFILE

Kedar Khare
Indian Institute of Technology Delhi
151 PUBLICATIONS **998** CITATIONS
SEE PROFILE

Research Article | Vol. 25, No. 15 | 24 Jul 2017 | OPTICS EXPRESS 17524
Optics EXPRESS

Robust laser beam engineering using polarization and angular momentum diversity

PRIYANKA LOCHAB, P. SENTHILKUMARAN, AND KEDAR KHARE*

Department of Physics, Indian Institute of Technology Delhi, New Delhi 110016, India
**kedark@physics.iitd.ac.in*

Abstract: We describe a laser beam engineered to carry $l = 0$ and $l = 1$ orbital angular momentum (OAM) states in orthogonal polarizations. It is observed that on collinear transmission through a random phase screen, the far field diffraction intensity patterns for the individual polarization states are complementary with significant negative correlation. As a result the combined intensity profile for the beam remains robust against time varying phase fluctuations. In our simulation and experiment the SNR for the central lobe of the combined far-field diffraction pattern defined as mean divided by the standard deviation of intensity values shows significant improvement over that for individual polarizations. The concept of polarization and OAM diversity as demonstrated here can be considered valuable for robust laser beam engineering without the requirement of any active real-time correction methods.

OCIS codes: (050.4865) Optical vortices; (010.1300) Atmospheric propagation; (030.6140) Speckle; (030.7060) Turbulence; (260.5430) Polarization.

References and links

1. Yu A Kravtsov, "Propagation of electromagnetic waves through a turbulent atmosphere," Rep. Prog. Phys. **55**, 39–112 (1992).
2. H. T. Eyyuboglu, "Propagation of higher order Bessel-Gaussian beams in turbulence," Appl. Phys. B **88**, 259–265 (2007).
3. P. Birch, I. Ituen, R. Young and C. Chatwin, "Long-distance Bessel beam propagation through Kolmogorov turbulence," J. Opt. Soc. Am. A **32**, 2066–2073 (2015).
4. H. T. Eyyuboglu, "Annular, cosh and cos Gaussian beams in strong turbulence," Appl Phys B **103**, 763–769 (2011).
5. Y. Cai, "Propagation of various flat-topped beams in a turbulent atmosphere," J. Opt. A: Pure Appl. Opt. **8**, 537–545 (2006).
6. Z. Bouchal, "Resistance of nondiffracting vortex beam against amplitude and phase perturbations," Opt. Comm. **210**, 155–164 (2002).
7. G. Gbur and R. K. Tyson, "Vortex beam propagation through atmospheric turbulence and topological charge conservation," J. Opt. Soc. Am. A **25**, 225–230 (2008).
8. D. J. Sanchez and D. W. Oesch, "Orbital angular momentum in optical waves propagating through distributed atmospheric turbulence," Opt. Express **19**, 24596–24068 (2011).
9. M. Salem, T. Shirai, A. Dogariu and E. Wolf, "Long-distance propagation of partially coherent beams through atmospheric turbulence," Opt. Comm. **216**, 261–265 (2003).
10. W. Cheng, J. W. Haus and Q. Zhan, "Propagation of vector vortex beams through a turbulent atmosphere," Opt. Express **17**, 17829–17836 (2009).
11. O. Korotkova and E. Wolf, "Changes in the state of polarization of a random electromagnetic beam on propagation," Opt. Comm. **246**, 35–43 (2005).
12. J. D. Barchers and D. L. Fried, "Optimal control of laser beam for propagation through a turbulent medium," J. Opt. Soc. Am. A **19**, 1779–1793 (2002).
13. T. Weyrauch and M. A. Vorontsov , "Free-space laser communications with adaptive optics: Atmospheric compensation experiments," J. Opt. Fiber. Commun. Rep. **1**, 355–379 (2004).
14. K. G. Larkin, D. J. Bone and M. A. Oldfield, "Natural demodulation of two-dimensional fringe patterns. I. General background of the spiral phase quadrature transform," J. Opt. Soc. Am. A **18**, 1862–1870 (2001).
15. K. Khare, "Complex signal representation, Mandel's theorem, and spiral phase quadrature transform," Appl. Opt. **47**, E8–E12 (2008).
16. D. P. Ghai, P. Senthilkumaran and R. S. Sirohi, "Single-slit diffraction of an optical beam with phase singularity," Opt. Lasers Eng. **47**, 123–126 (2009).
17. J. Hickmann, E. Fonseca, and S. Chavez Cerda, "Unveiling a truncated optical lattice associated with a triangular aperture using light's orbital angular momentum," Phys. Rev. Lett. **105**, 053904 (2010).
18. S. Singh, A. Ambuj and R. Vyas,"Diffraction of orbital angular momentum carrying optical beams by a circular aperture," Opt. Lett. **39**, 5475–5478 (2014).

#291329 https://doi.org/10.1364/OE.25.017524
Journal © 2017 Received 23 Mar 2017; revised 28 Jun 2017; accepted 2 Jul 2017; published 12 Jul 2017

Optics EXPRESS

19. M. K. Sharma, C. Gaur, P. Senthilkumaran and K. Khare, "Phase imaging using spiral-phase diversity," Appl. Opt. **54**, 3979–3985 (2015).
20. S. Echeverri-Chacón, R. Restrepo, C. Cuartas-Vélez and N. Uribe-Patarroyo, "Vortex-enhanced coherent-illumination phase diversity for phase retrieval in coherent imaging systems," Opt. Lett. **41**, 1817–1820 (2016).
21. E. Karimi, G. Zito, B. Piccirillo, L. Marrucci and E. Santamato, "Hypergeometric-Gaussian modes," Opt. Lett. **32**, 3053–3055 (2007).
22. E. Karimi, B. Piccirillo, L. Marrucci and E. Santamato, "Light propagation in a birefringent plate with topological charge," Opt. Lett. **34**, 1225–1227 (2009).
23. G. Vallone, "On the properties of circular beams: normalization, Laguerre-Gauss expansion, and free-space divergence," Opt. Lett. **40**, 1717–1719 (2015).
24. A. M. Beckley, T. G. Brown, and M. A. Alonso, "Full Poincare beams," Opt. Express **18** 10777–10785 (2010).
25. E. J. Galvez, S. Khadka, W. H. Schubert, and S. Nomoto, "Poincare-beam patterns produced by nonseparable superpositions of Laguerre-Gauss and polarization modes of light," Appl. Opt. **51**, 2925–2934 (2012).
26. F. Cardano, E. Karimi, L. Marrucci, C. de Lisio, and E. Santamato, "Generation and dynamics of optical beams with polarization singularities," Opt. Express **21**, 8815–8820 (2013).
27. S. K. Pal, Ruchi and P. Senthilkumaran, "C-point and V-point singularity lattice formation and index sign conversion methods," Opt. Commun. **393**, 156–168 (2017).
28. J. W. Goodman, "Statistical properties of laser speckle patterns," in *Laser Speckle and Related Phenomena*, J. C. Dainty, ed. (Springer, 1975).
29. E. M. Johansson and D. T. Gavel, "Simulation of stellar speckle imaging," Proc. SPIE **2200**, 372–383 (1994).
30. B. R. Frieden, *Probability, Statistical Optics, and Data Testing* (Springer, 2001).

1. Introduction

Propagation of optical beams through a random fluctuating medium such as earth's atmosphere is an important topic for applications such as free space optical communication and defense systems where it is required to deliver a well-defined beam spot onto a receiver or a specific target. The quality of an optical beam propagating through atmosphere degrades due to time-varying inhomogeneities in refractive index and scattering by particulates leading to scintillations, beam spreading and beam wandering. Our aim in this paper is to introduce a novel approach for generating a laser beam whose intensity profile is robust against time varying phase fluctuations so that it can be used for faithful beam delivery. We achieve this by using the concept of simultaneous polarization and OAM diversity in the beam. This approach does not require any active correction mechanism such as adaptive optics.

Laser beam propagation through atmosphere is an extensively studied topic [1] and the propagation characteristics of several kinds of beams such as Bessel [2, 3], cos and cosh-Gaussian [4], flat-topped [5], and vortex carrying beams [6–8] are known. It has been shown that partially coherent [9] and inhomogeneously polarized [10] beams are less affected by atmospheric turbulence in comparison to homogeneously polarized scalar beams. The changes in the polarization state of optical beams due to turbulence have also been described [11]. While these studies have provided important insights for designing systems requiring laser beam propagation through atmospheric turbulence, it is generally believed that an active real time correction system employing adaptive optics is required [12, 13] for maintaining the desired beam quality.

Our approach to engineering an optical beam that is robust to random phase fluctuations is based on designing orthogonal polarization states of the beam that evolve in a complementary manner on passing through turbulence. In case of 1D signals, the sines and cosines having complementary maxima and minima are connected by the Hilbert transform. The optimal extension of the Hilbert transform concept to 2D is known as the spiral phase quadrature transform [14, 15]. In particular for a 2D signal $g_1(x, y)$, a quadrature $g_2(x, y)$ may be obtained using the spiral phase transform as:

$$g_2(x, y) = \mathcal{F}^{-1}\{\exp(i\phi)\mathcal{F}\{g_1(x, y)\}\}. \tag{1}$$

Here $\mathcal{F}$ and $\mathcal{F}^{-1}$ denote the forward and inverse 2D Fourier transform operations and ϕ is the polar angle in the 2D Fourier space. As shown in [14, 15], the two signals $g_1(x, y)$ and

Optics EXPRESS

$g_2(x, y)$ show sine-cosine like complementarity. This complementarity has been reported in recent experiments on Fraunhoffer diffraction of various apertures illuminated with beams in $l = 0$ and $l = 1$ OAM states [16–18]. The OAM diversity has also found application to non-interferometric phase retrieval [19, 20]. In the present work we design a vector beam such that its two orthogonal polarization components are in $l = 0$ and $l = 1$ OAM states. When propagated collinearly through a randomly fluctuating phase screen, the diffraction intensity patterns corresponding to the two polarization states are complementary and therefore the overall intensity of the beam shows a well-defined central lobe.

This paper is organized as follows. In Section **2** we describe the nature of the inhomogeneously polarized beam that we use and a nominal experimental setup. Simulations and experimental results on the diffraction patterns observed when this beam is passed through random phase screens are shown in Section **3**. Finally in Section **4** we provide concluding remarks.

2. Optical beam with polarization and OAM diversity

Consider an optical beam propagating in the $+z$ direction having a transverse E- field profile in the $z = 0$ plane as described by:

$$\vec{E}(x, y) = \frac{1}{\sqrt{2}}[\hat{x} + e^{i\theta}\hat{y}]\psi(x, y). \tag{2}$$

Here $\hat{x}$ and $\hat{y}$ are unit vectors in x and y directions respectively, $\theta = \arctan(y/x)$ is the polar angle in the transverse $x - y$ plane and the function $\psi(x, y)$ represents the normalized beam profile function (e.g. the fundamental Gaussian mode). A time-dependence of the form $\exp(-i\omega t)$ is assumed. The x and y-components of the field are seen to be in the $l = 0$ and $l = 1$ OAM states respectively. This field profile may be generated by an arrangement shown in Fig.

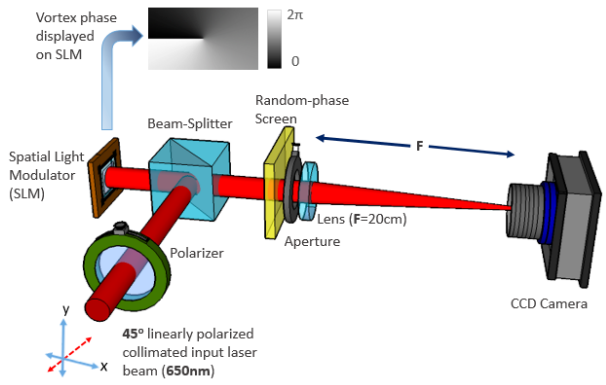

Fig. 1. Experimental setup for generating the proposed vector beam and observing effect of its propagation through a random phase screen.

1. The liquid crystal Spatial Light Modulators (SLMs) are sensitive to p-polarized light and act like a plane mirror for the s-polarized light. So when a 45-degree linearly polarized laser beam ($\lambda = 650$ nm, beam diameter = 1 cm at collimating lens which is 20 cm away from the SLM) is sent onto the SLM device (Make: Holoeye, Model: LETO) displaying a charge-1 spiral phase pattern, the composite beam in the SLM plane is approximately in the form described by Eq. (2). The y-polarized component of the beam that is reflected from the SLM is known to be in the generalized circular or Hypergeometric Gaussian form [21–23]. The resultant beam is passed through a random phase screen followed by a lens ($F = 20$ cm). The lens aperture (diameter =

Optics EXPRESS

1.5 mm) is selected so that the individual speckles in the intensity pattern observed in the back focal plane of the lens could be adequately sampled by CCD sensor pixels (Make: Lumnera, Model: Infinity 2-1R, pixel size = 4.65μm). The polarizer in the setup is used for observing intensity patterns for individual polarizations. Denoting the random phase screen in the lens aperture by the transmission function $s(x, y)$, the total intensity observed on CCD sensor in the back focal plane of the lens can be described as:

$$I_{\text{Total}} = |\mathcal{F}\{s(x,y)E_x(x,y)\}|^2 + |\mathcal{F}\{s(x,y)E_y(x,y)\}|^2, \tag{3}$$

where E_x and E_y are the x and y components of the field in the random phase screen plane. It may be noted from Eq. (1) and Eq. (3) that the E-fields corresponding to the x and y polarization components in the sensor plane essentially have a 2D Hilbert transform relationship due to the OAM diversity in E_x and E_y.

The state of polarization of the beam at the SLM plane and after nominal propagation (z = 40 cm) is shown in Figs. 2(a) and 2(b) respectively. On propagation from SLM plane the resultant inhomogeneously polarized beam contains a C-point polarization singularity structure in the form of a lemon-star dipole [24–27] as shown in Fig. 2(b) where the background colormap represents the total beam intensity.

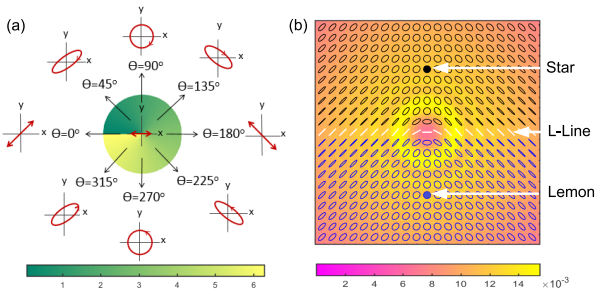

Fig. 2. State of polarization of the proposed vector beam (a) at the SLM plane and (b) after propagation over z = 40 cm from SLM. Colormap in (a) shows phase difference between E_x and E_y. Background in (b) shows simulated total beam intensity at z = 40 cm from SLM. The black and blue colours in (b) represent opposite handedness. The polarization singularity features such as lemon, star and L-line are also marked.

3. Simulation and experimental results

In this Section, we present simulation and experimental results to illustrate the behavior of the above beam on passing through a random phase screen. The simulation is performed with the parameters in the experimental setup in Fig. 1. A random medium like atmosphere at a given instant can be described by a phase screen in the lens aperture [28]. In order to generate the phase screen, we start with a random phase function in the lens aperture with phase distributed uniformly in $[0, 2\pi]$. This random phase function is convolved with an averaging Gaussian filter to induce correlation over phase fluctuation length scale [29] such that the average spot size on the sensor in simulation is made equal to that observed in our experiment. For experimental demonstration, we used different positions of a crumpled polythene sheet as random phase object in the lens aperture. The simulation and experimental results in Figs. 3 and 4 are based on 50 realizations of the random phase screen each. Figures 3(a)-3(c) show three of the simulated phase screens and Figs. 3(d)-3(l) show simulated intensity patterns in the sensor plane for individual polarizations as well as the combined intensity patterns. The corresponding experimental intensity records are shown in Figs. 4(a)-4(p) where Figs. 4(a)-4(d)

Optics EXPRESS

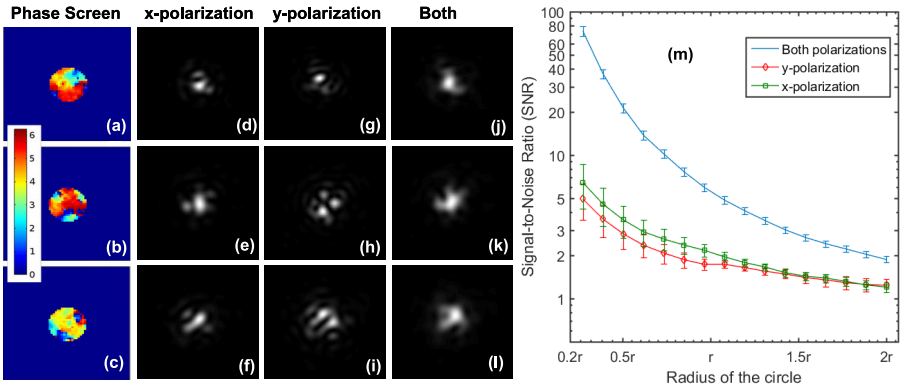

Fig. 3. Simulated intensities for propagation of the vector beam through a random phase screen. (a-c): phase maps for random phase screens in the lens aperture, corresponding intensity patterns in the sensor plane for (d-f): x-polarization ($l = 0$ OAM state), (g-i): y-polarization ($l = 1$ OAM state), (j-l): both polarizations together, (m) plot of SNR values vs. radius of circular region used for SNR calculation where r represents the radius of diffraction-limited spot (error bars represent standard deviation for 50 realizations of the random phase screen).

show data when no phase screen was used. We observe that the simulation and experiment demonstrate complementary intensity patterns for individual polarizations and improved beam profile when both the polarizations are present together. Based on 50 realizations of the random phase screen, the correlation coefficient [30] for the individual simulated polarization intensity images is observed to be equal to -0.95 ± 0.04. The corresponding correlation coefficient for experimental data is observed to be -0.71 ± 0.08 indicating significant negative correlation in the individual polarization intensities. A region of size equal to the diffraction-limited spot size and centered on the peak of the combined pattern was used for calculating the correlation coefficient.

In order to study the beam quality improvement quantitatively in both simulation and experiment, we selected a circular region centered on the peak intensity position for the combined intensity pattern and calculated the signal-to-noise ratio (SNR) of the beam defined as mean intensity divided by standard deviation of pixel values in the circular region. The SNR values for the corresponding circular regions in the individual polarization records were also evaluated for comparison. The plots in Figs. 3(m) and 4(q) show SNR variation as a function of the radius of the circular region used for the SNR calculation. The parameter r on the x-axis of SNR plots represents the radius of the diffraction limited spot. The error bars in these plots represent the standard deviation of the SNR values calculated over 50 realizations of the random phase screen. The SNR values for the combined beam are consistently greater than those for the individual polarizations. While the detailed statistics of the simulated phase screens and those corresponding to different regions of the crumpled polythene sheet is likely to be different, the trend in the SNR values for the simulations and experiments is very similar. When a beam is to be delivered through a randomly fluctuating medium such as atmosphere, the SNR plots as in Fig. 3(m) and Fig. 4(q) are useful for deciding the size of the receiver, so that, a significantly higher quality beam is received on the detector. The circular regions for SNR calculations are centered on peak position of combined beam intensity since this is the best position for the detector. Also this choice takes care of any beam wandering effects.

An important advantage of our method is that even if the random phase screen is time-varying,

Optics EXPRESS

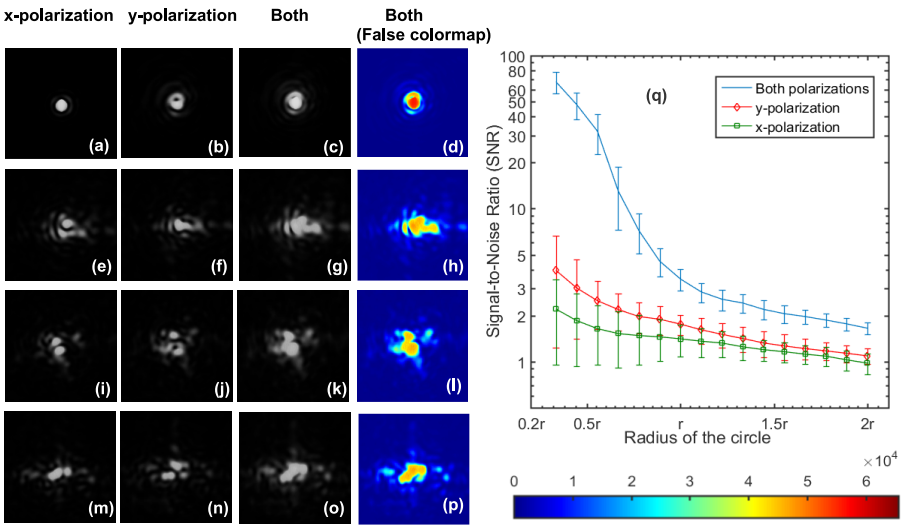

Fig. 4. Experimentally recorded intensities (individual polarizations and combined) for the proposed beam after passing through random phase screens in lens aperture (see Fig. 1). Phase screens used are (a)-(d): open aperture, (e)-(p): three distinct areas of crumpled polythene sheet. (q) variation of SNR as a function of the radius of the circular area used for SNR calculation (error bars represent standard deviation for 50 realizations of the random phase screen), False colormap for displaying the recorded CCD images is also shown.

the robustness of the central lobe in the combined intensity pattern holds without requirement of any real-time wavefront sensing and correction. For example, the different realizations of the random phase screens can be considered as appearing in the lens aperture as a time domain sequence and the SNR improvement results will still be valid.

4. Conclusion and future work

We have demonstrated a methodology for generating a laser beam using polarization and OAM diversity that is robust against time varying phase fluctuations. The central idea used in our approach is that the diffraction intensity patterns produced when two OAM states ($l = 0$ and $l = 1$) illuminate a given phase screen are complementary in nature. The two OAM states in orthogonal polarizations when passed collinearly through a randomly fluctuating phase screen therefore lead to a well-defined central intensity lobe without the need of any real-time wavefront correction via a feedback mechanism. Our simulation and experimental results on multiple realizations of random phase screens indicate significant improvement in the SNR of the central-lobe of the beam. We plan to study the propagation of the proposed beam and its generalizations through different types of random media in future.